공학석사 학위논문

# Drying behavior and rheological properties of Li-ion anode model slurries at different pH

# 음극 리튬 이온 전지 슬러리의 pH에 따른 유변학 및 건조 거동 연구

**2019 년 2 월**

서울대학교 대학원
화학생물공학부
정 민 환

공학석사 학위논문

# Drying behavior and rheological properties of Li-ion anode model slurries at different pH

# 음극 리튬 이온 전지 슬러리의 pH에 따른 유변학 및 건조 거동 연구

**2019 년 2 월**

서울대학교 대학원
화학생물공학부
정 민 환

# 음극 리튬 이온 전지 슬러리의 pH에 따른 유변학 및 건조 거동 연구

지도교수 안 경 현

이 논문을 공학석사 학위논문으로 제출함

**2019 년 2 월**

서울대학교 대학원
화학생물공학부
정 민 환

정민환의 석사 학위논문을 인준함

**2019 년 2 월**

위 원 장 이 원 보 (인)
부 위 원 장 안 경 현 (인)
위 원 남 재 욱 (인)

# Abstract

# Drying behavior and rheological properties of Li-ion anode model slurries at different pH

Jeong, Min Hwan
School of Chemical and Biological Engineering
The Graduate School
Seoul National University

Lithium-ion batteries have a lot of advantages such as a high energy density and a long cycle life. With respect to the electrode process, research has been conducted to improve the electrode performance by modifying the particles, to optimize the process by changing the parameters of the unit process, or to control the rheological properties by changing the composition ratio and interaction of each component in the slurry state. However, based on the interaction between the polymeric binder and the active material, few studies have been developed on the relationship between the slurry state and the microstructure after drying. In this study, we investigated the influence of the pH-dependent adsorption on the drying behavior and the microstructure after drying in an aqueous anolyte slurry using poly (acrylic acid) (PAA) as a polymeric binder.

After the pH of the slurry based on PAA and graphite, which is a microsized active material, was adjusted to 3, 7, and 11, respectively, the amount of adsorption was

measured. The amount of adsorption was found to be zero. After confirming the existence of interaction difference by the adsorption measurement, each slurry was evaporated under a certain condition, and the difference in drying behavior was confirmed. When the pH was 11, the peaks occurred in the middle of drying and the occurrence of this peak was due to capillary stress. On the other hand, it was confirmed that only the maximum plateau region due to polymer shrinkage existed in the slurry having lower pH. In the porosity measurement to determine the microstructure after drying, it was corroborated that the electrode fabricated from the slurry of pH 11 had nano-sized pores as well as lower porosity than the other slurries. Adjusting the degree of adsorption of the electrode slurry affects the drying process and the microstructure of the electrode.

**Key words: anode slurry, adsorption, drying stress, microstructure**

***Student Number*: 2017-27364**

# Contests

# List of Figures

# Chapter 1.

# Introduction

Lithium-ion battery has many benefits like high energy density and long cycle life, and its necessity becomes increased recently. Battery slurries are composed of micro-sized particles as an active material, nano sized particles as a conductive agent, a polymeric binder, and solvent. Much research has been investigated with regard to enhancing electrochemical properties by modifying particles [1-4]. Rheological properties of the battery slurries and a unit process of battery industry as well as increasing electrochemical properties have been addressed for major issues. Because of consuming enormous energy and its dynamic phase change [5], the attempts of focusing on drying process, which is one of the unit processes have been developed. For example, overcoming a coffee ring effect caused by inhomogeneity in the suspension [6], binder migration during evaporating solvent [7], and controlling processing variations [8] are addressed. Many papers have been researched about characterizing mechanical properties by changing the interaction between components: the interaction between the conductive agent and polymeric binder [9, 10], the affinity [11] and volume fraction ratio [12] between particles, and the interaction between the active material and polymeric binder [13]. It is conducted that optimal processing conditions are suggested by measuring *in-situ* drying stress in accordance with the concentration of styrene butadiene rubber (SBR) and carboxymethyl cellulose (CMC) in the battery slurries by Lim et al [14].

However, few attempts have focused that the drying process may be affected to the different interaction between the micro sized particles and the polymeric binder. In this study, the rheological properties and drying behavior were investigated by means of adjusting pH in order to change the interaction between graphite as the active material, and poly(acrylic acid)

(PAA) as the polymeric binder.

On the basis of this criteria, it was confirmed that the interaction at the battery slurries contained with linear PAA and graphite was dependent on pH by measuring the amount of adsorption. In an aspect of drying behavior, we characterized the drying behavior by means of *in-situ* drying stress measurement as previous research [15, 16]. The changed interaction would have influenced the drying behavior with cross-linked PAA to some extent.

# Chapter 2.

# Experimental methods

2.1 Materials and sample preparation

The active material was natural graphite (SG-BH8, Ito Graphite Co., Ltd., Japan) with a density of 2.23 g/cm³, average diameter of 8.1 μm and a specific surface area of 12.12 m²/g. PAA was used as polymeric binder and, in this study, two types of PAA were used: linear polymer (Molecular weight = 250,000 g/mol) and cross-linked polymer (Molecular weight = 1,250,000 g/mol). Cross-linked PAA aqueous solution was prepared by dissolving 1 wt% PAA in deionized water with propeller type stirrer at 1,000 rpm (rotations per minute) for 3 hours. Linear PAA-water solution was prepared by diluting 35 wt% PAA with a magnetic stirrer for 2 hours. Every polymer concentration in the model slurries was 1 wt%. Prepared PAA aqueous solution and NaOH 2M solution were mixed with 45 wt% graphite particles in order to adjust pH 3, 7, and 11. The slurries were stirred with planetary mixer at 2,000 rpm for 5 minutes and overhead stirrer at 1,000 rpm for 5 minutes. Finally, they were combined with additional water by the planetary mixer at 2,000 rpm for 5 minutes.

2.2. Experimental set-up

2.2.1. Rheological characterization

In terms of the slurries with cross-linked PAA, the rheological characterization was performed by AR-G2 (TA Instruments, United States) rotational rheometer at 25 ℃ with a cross-hatched parallel plate of 40 mm in diameter. All slurries were taken 2 minutes of a rest time in order to get rid of shear history that may have appeared during loading of the slurry. Viscosity was measured by steady-shear rate sweep test from shear rate 0.1 $s^{-1}$ to 100 $s^{-1}$. To obtain the modulus of the slurries, frequency sweep test was performed from 0.1 rad/s to 100 rad/s in the linear viscoelastic regime.

At the slurries with linear PAA, the geometries of the parallel plate of 60 mm and 40 mm in diameter were used at 25 ℃. The slurry at pH 11 was taken 2 minutes of a rest time while the slurries at pH 3 and 7 were not taken the rest time as a result of sedimentation of graphite. Viscosity was determined by steady-shear rate sweep test from shear rate 0.1 $s^{-1}$ or 1 $s^{-1}$ to 100 $s^{-1}$. Frequency sweep measurement was performed from frequency 1 rad/s to 100 rad/s in linear viscoelastic regime identified by the strain sweep test.

2.2.2. Adsorption measurement

The amount of PAA adsorbed on graphite was estimated as functions of linear PAA concentration. The samples with 20 wt% graphite and various concentrations of the linear PAA were produced and the supernatant was extracted after the samples were centrifuged at 10,000 rpm until graphite had completely separated from the supernatant. The amount of PAA adsorbed on the graphite was calculated by measuring the concentration of non-adsorbing PAA in the supernatant.

2.2.3. Sedimentation characterization

A turbimetric method is performed to quantify sedimentation, more specifically, tendency transmission (T) and backscattering (BS) curves are measured. It was able to measure the stability of opaque colloidal dispersions and to detect instability phenomena. In this work, the analysis of stability for the slurries was performed as back-scattering (ΔBS) profiles.

2.2.4. Drying stress measurement

The drying stress was calculated using a cantilever deflection method and the apparatus are comprised of a cantilever, position sensing detector, laser, and data acquisition. The slurries were coated on the cantilever, and it was deflected in the middle of drying as a result of developing in-plane tensile stress.

The degree of deflection of the coated cantilever is detected by the position sensing detector. Silicon wafer of 70 mm × 6 mm with approximately 530 μm of thickness was prepared as the cantilever, or the substrate. The silicon wafer was coated by titanium and gold by sputtering to enhance laser

deflection.

Critical crack thickness (CCT) is defined by the thickness above which cracks are created at the surface [17]. In this study, the slurries were coated by doctor blade coater at 300 μm, 200 μm, and 150 μm in order to characterize CCT, and 150 μm was below CCT. Therefore, every initial coating thickness was 150 μm. The drying environments were maintained at 25±1 ℃ and at 30±1 % of relative humidity. The degree of cantilever deflection was converted to the drying stress by appling the Cocoran equation [18]:

$$\sigma = \frac{d E t_s^3}{3 t_c l^2 (t_s + t_c)(1-\nu)} + \frac{d E_c (t_s + t_c)}{l^2 (1-\nu_c)}$$

where d, t, l, E, and ν are the degree of deflection, thickness, substrate length, elastic modulus, and Poisson ratio, respectively and subscripts s and c mean the substrate and film after, respectively. When the modulus of the substrate, $E_s$, is considerably larger than that of the film, $E_s$, the second term is allowed to be ignored as previous research [9, 10].

# Chapter 3.

# Results and discussion

3.1. Slurry-state properties

It was apparent beforehand that the suspensions with linear PAA and $LiCoO_2$, which are micro-sized particles, shifted rheological properties [19]. According to the previous attempt, our slurries may have seen changed rheological behavior depending on pH. Figure 3-1 shows the rheological properties of linear PAA solution, graphite suspension, and the suspension containing both linear PAA and graphite.

In the case of 1 wt% linear PAA solution, Newtonian behavior was shown for the entire range of the shear rate regardless of pH. Shear thinning and yielding behavior were exhibited at 45 wt% graphite suspension for the entire range of the shear rate without regard to pH. Their magnitudes of viscosity were almost the same. However, different viscosity curves were exhibited at different pH when PAA and graphite were mixed. The slurry at pH 11 showed shear thinning behavior and its magnitudes of viscosity were similar to that of graphite suspension. Therefore, it could be assumed that the interaction between PAA and graphite was varied at different pH as the previous research [19].

In order to confirm the degree of the interaction, adsorption measurement was accomplished. Figure 3-2 provides the amount of adsorption at different pH. As can be seen, the graphite did not adsorb PAA at pH 11 and the amount of adsorption was increased with decreasing pH. It is well known that the pKa of PAA is approximately 4.2 [20] and the concentration of the ionized form ($COO^-$) rises as increasing pH. In conclusion, at pH 7 or more, PAA was not adsorbed onto the graphite because the particle took the negative charge. The different amount of adsorption dependent on pH affected sedimentation judging from backscattering result. According to the

backscattering results, at pH range from 3 to 7, sedimentation of graphite occurs clearly in the model slurries while sedimentation was rarely observed at pH 11.

In conclusion, when the linear PAA was used as the polymeric binder, rheological behavior, the amount of adsorption, and sedimentation were varied at pH of the model slurries.

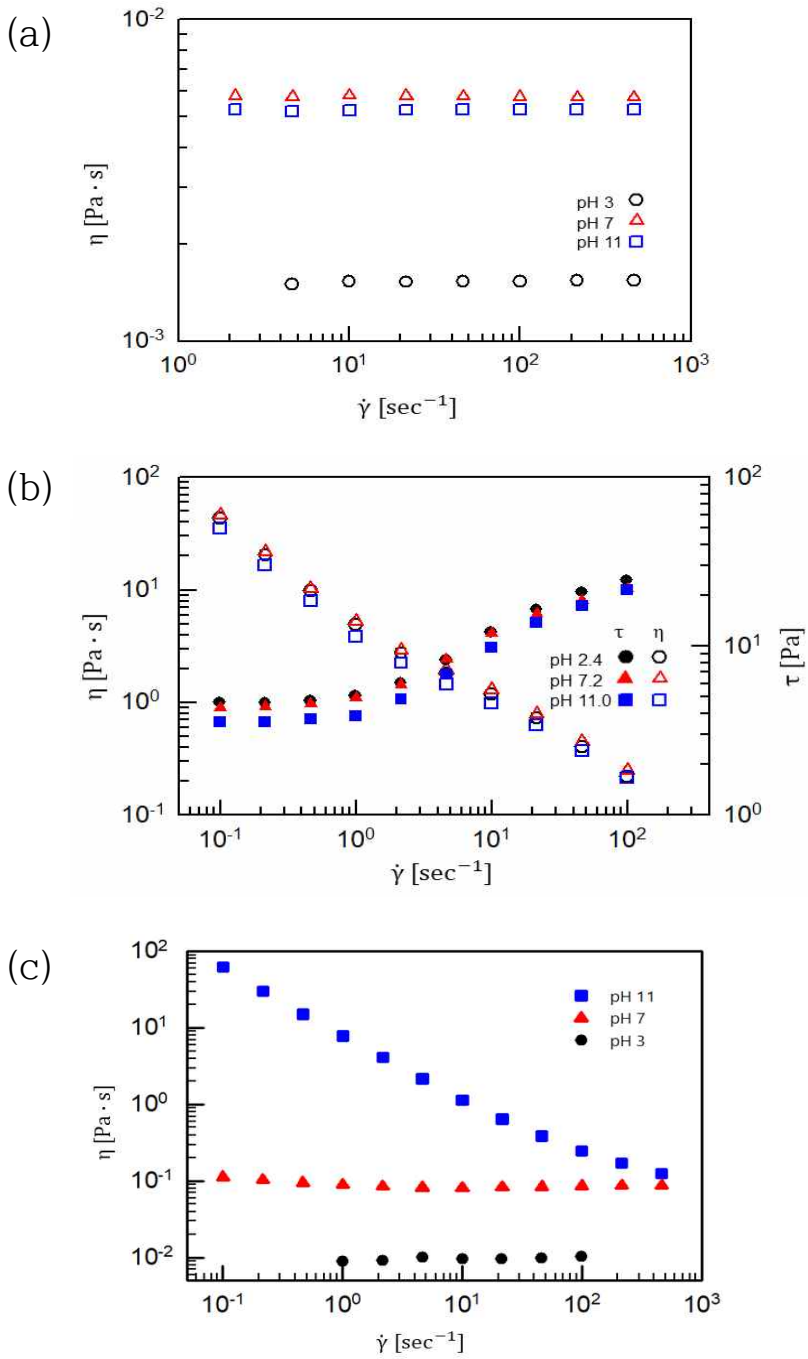


Figure 3-1. Rheological properties of (a) 1 wt% linear PAA solution, (b) 45 wt% graphite solution, and (c) 1 wt% linear PAA and 45 wt% graphite suspension at different pH.

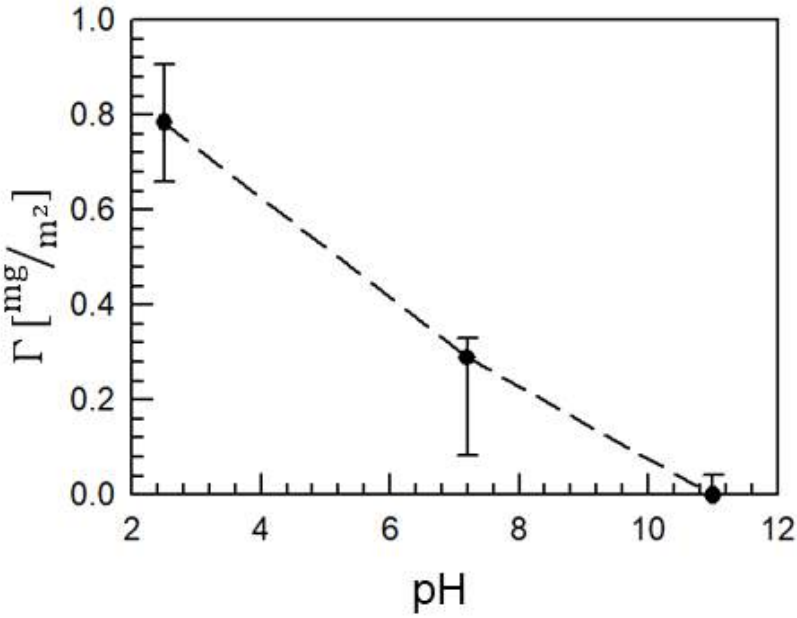


Figure 3-2. The amount of adsorption at different pH.

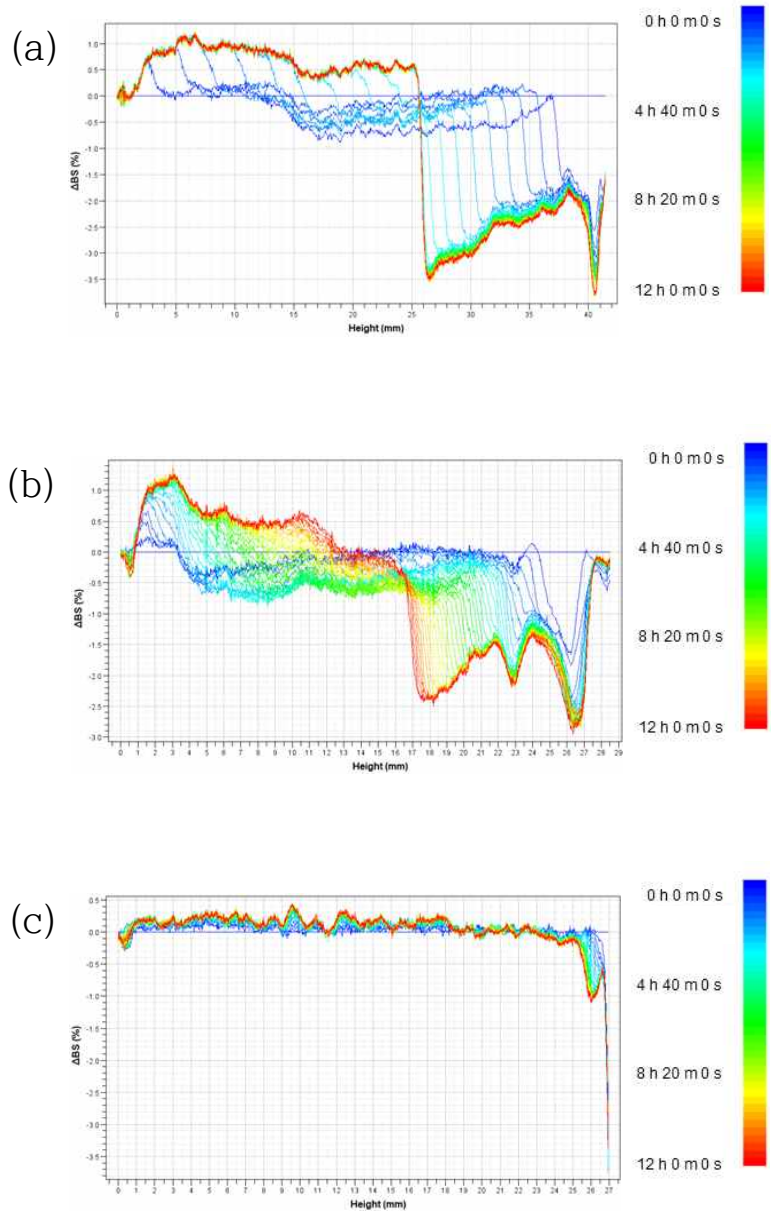


Figure 3-3. Sedimentation results of (a) pH 3, (b) pH 7, and (c) pH 11.

However, when the electrodes are fabricated, the polymeric binder has higher viscosity and takes elastic modulus such as cross-linking PAA. In the case of the cross-linked PAA solution, shear thinning and yielding were exhibited for the entire range of the shear rate different with the linear PAA solution (see Figs. 3-4(a)). And their magnitudes were larger than that of the linear PAA solution. Not only the cross-linked PAA solution but also the model slurries with cross-linked PAA were shown shear thinning and yielding for the entire range of the shear rate. Although the different extent of viscosity and modulus was shown between pH 3 and 7, little difference was exhibited between pH 7 and 11 which showed the distinct amount of adsorption (see Fig. 3-2). Therefore, in this study, *in-situ* drying stress measurement may be required so as to characterize the properties at the distinct amount of adsorption.

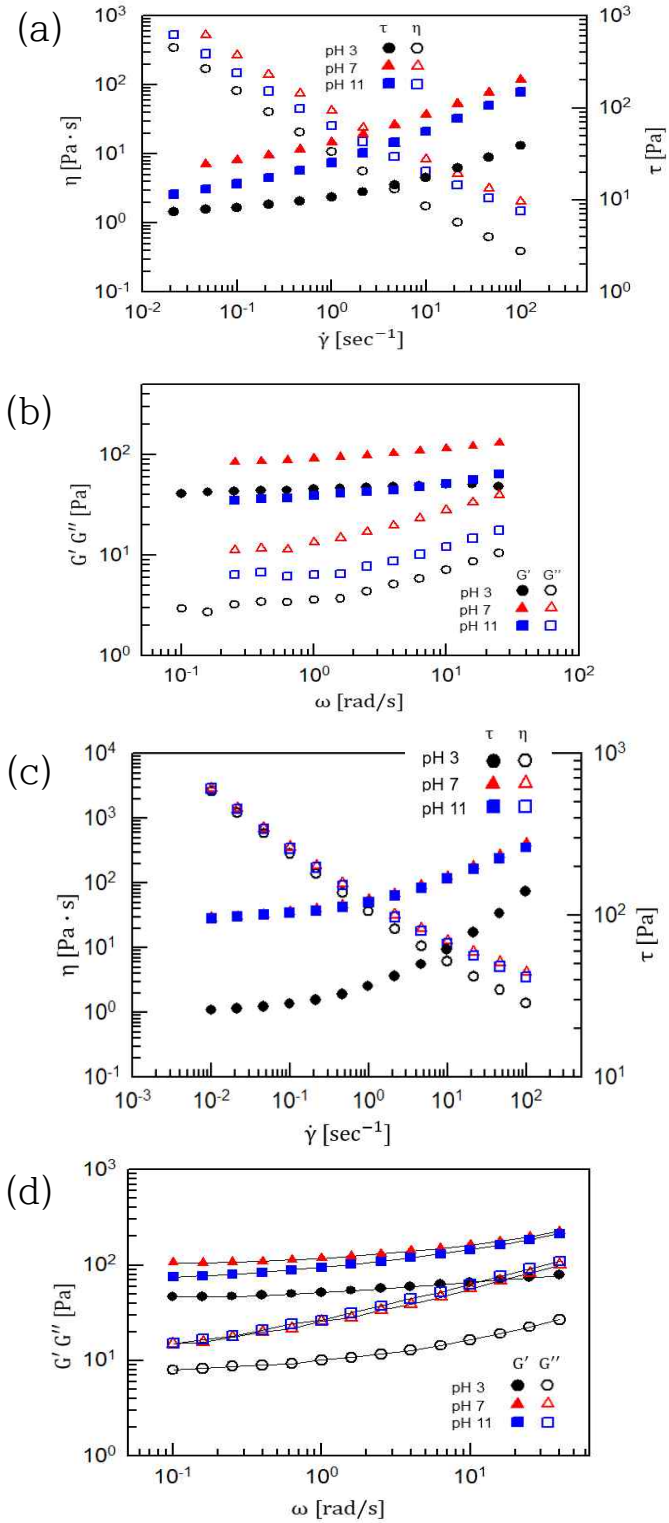


Figure 3-4 (a) and (b) are viscosity and modulus of cross-linked PAA solution, respectively, and (c) and (d) are viscosity and modulus of the model slurries with the cross-linked PAA, respectively.

3.2. Drying stress measurement

As discussed previously, a peak and a maximum plateau region were shown in the drying stress measurement of suspensions contained polymer and particle [21]. It was known that the peak resulted from capillary pressure ($P_{ca}$) at the meniscus and that the magnitude of the peak was calculated by Young-Laplace equation [22].

$$P_{ca} = \frac{2\gamma \cos\theta}{r_p}$$

$\gamma$, $\theta$, and $r_p$ are liquid vapor surface tension, liquid solid contact angle, and equivalent pore radius, respectively. The equivalent pore radius can be estimated by the hydraulic radius, $r_h$, since the capillary pores in the particle network were barely similar to cylindrical tubes [23].

$$r_h = \frac{2(1-\phi)}{\phi \rho_s S}$$

$\phi, \rho_s$ and S are the particle volume fraction, the density of the solid phase, and surface area of particles, respectively.

Figure 3-5 displays the drying stress and weight loss curve at different pH. According to figure 3-5, one peak was exhibited at pH 11 and the value was at about 0.17 MPa while the suspensions at pH 3 and 7 did not show the peak. It was corroborated by previous research [24] that no peak was displayed when the graphite fully adsorbed the polymer.

However, when PAA was not adsorbed to the graphite, the previous research [24] may not have suggested the extent of the capillary pressure. At pH 11, the contact angle and surface tension were about 80 ° and 62.5 mN/m, respectively, and then the extent of capillary stress was 0.16 MPa which was the acceptable result because the error range of this study was

±0.03 MPa.

When the surface tension was measured, the polymer solution was diluted from 1 wt% to 0.13 wt% in order to make droplet suitable shape. It might be some errors, however, as discussed previously [25], above 800 ppm, a minor difference was showed.

Therefore, it can conclude that the drying stress behavior was dependent on the adsorption state; when the particle adsorbed the polymeric binder, no peak was shown while the non-adsorbing system showed one peak.

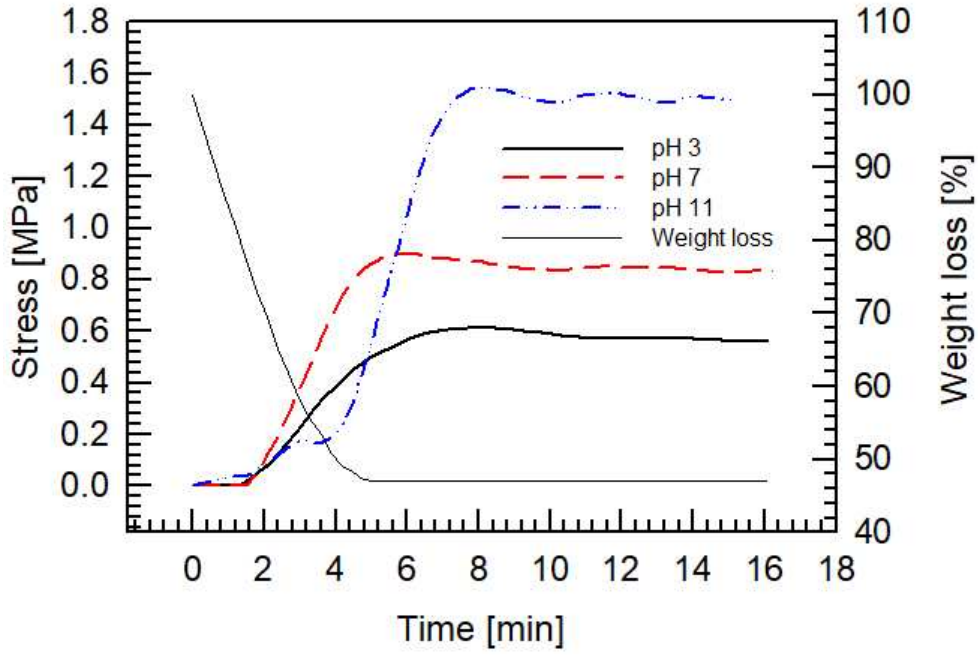


Figure 3-5. The drying stress behavior of the model slurries depending on pH.

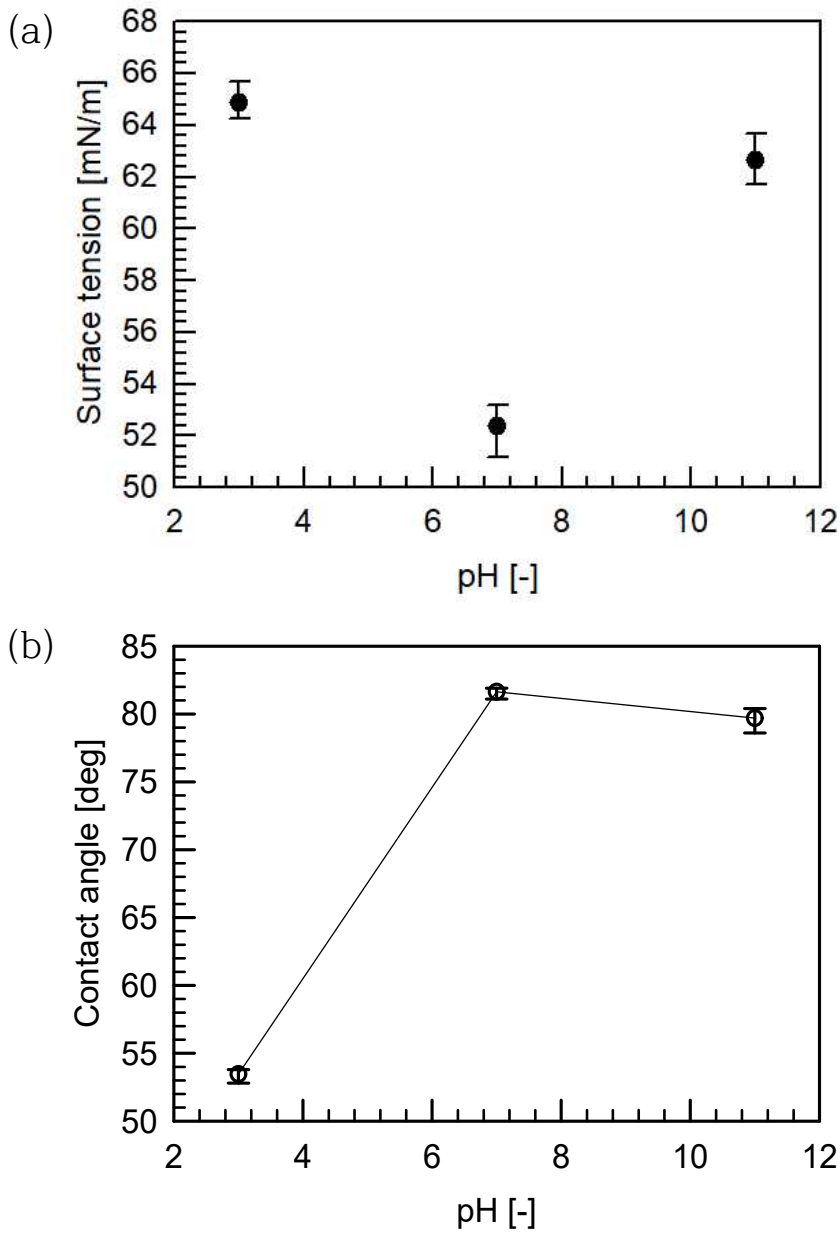


Figure 3-6. (a) Surface tension of cross-linked PAA 0.13 wt% and (b) equilibrium contact angle of cross-linked PAA 1 wt% on graphite plate.

# Chapter 4.

# Conclusion

Former work has documented that the optimal concentration of the polymeric binder is provided by analyzing drying stress behavior [14]. However, these studies have not focused on the interaction between the active material and the polymeric binder.

In this study, it was investigated that the drying behavior and the microstructure of dried electrodes were varied at depending on pH, which was related to the amount of adsorption. First, by using the linear PAA as the polymeric binder, it was confirmed that, above pH 7, the magnitude of adsorption pH was almost zero. It may have been indicated that it affected the drying behavior and the microstructure to some extent. More specifically, in the case of adsorbing the binder on the graphite, the capillary stress was not exhibited and more porous structures were acquired. However, in case of not adsorbing the binder on the graphite, capillary stress may have been exhibited judging from the results of the contact angle and the surface tension.

It may have been concluded that the proper range of pH must be considered when the battery slurries were fabricated since the drying behavior and the microstructure were affected by the amount of adsorption. The findings may also offer an understanding of implying electrochemical properties of the battery electrode.

# References


[1] X. Zhou, F. Wang, Y. Zhu, and Z. Liu, Graphene modified LiFePO4 cathode materials for high power lithium ion batteries, *Journal of Materials Chemistry*, vol. 21, pp. 3353-3358, 2011

[2] S. Hu, G. Cheng, M. Cheng, B. Hwang, and R. Santhanam, Cycle life improvement of ZrO2-coated spherical $LiNi_{1/3}Co_{1/3}Mn_{1/3}O_2$ cathode material for lithium ion batteries, *Journal of Power Sources*, vol. 188, 2, pp. 564-569, March 2009

[3] Y. S. Lee, and K. Y. Shem, Powder Technology , Fluidized bed , polymers , materials (inorganics, organics) : the electrochemical characteristics of surface modified graphite materials by Tin - oxide for Lithium secondary batteries, *Korean Chem. Eng. Res.*, vol. 40, 1, pp. 88-92, 2002

[4] E. Um, T. Lee, and C. Lee, Synthesis of Sn-GIC for carbon electrode of Lithium ion battery and its electrochemical characteristics, *Korean Chem. Eng. Res.*, vol. 18, 5, pp. 449-453, October 2007

[5] T. Kudra, Energy aspects in drying, *Drying Technology*, vol. 22, 5, pp. 917-932, 2004

[6] M. Majumder, C. S. Rendall, J. A. Eukel, James Y. L. Wang, N. Behabtu, C. L. Pint, T. Liu, A. W. Orbaek, F. Mirri, J. Nam, A. R. Barron, R. H. Hauge, H. K. Schmidt, and M. Pasquali, Overcoming the “Coffee-Stain” Effect by Compositional Marangoni-Flow-Assisted Drop-Drying, *Journal of Physical Chemistry B*, vol. 116, 22, pp. 6536-6542, 2012

[7] S. Lim, K. H. Ahn, and M. Yamamura, Latex migration in battery slurries during drying, *Langmuir*, vol. 29, 26, pp. 8233-8244, 2013

[8] S. Jaiser, M. Müller, M. Baunach, W. Bauer, P. Scharfer, and W. Schabel, Investigation of film solidification and binder migration during drying of Li-Ion battery anodes, *Journal of power sources*, vol. 318, pp. 210-219, June 2016

[9] S. Kim, J. H. Sung, K. Hur, K. H. Ahn, and S. J. Lee, The effect of adsorption kinetics on film formation of silica/PVA suspension, *Journal of Colloid and Interface Science*, vol. 344, 2, pp. 308-314, April 2010

[10] S. Kim, J. H. Sung, S. Chun, K. H. Ahn, and S. J. Lee, Adsorption‐stress

relationship in drying of silica/PVA suspensions, *Journal of Colloid and Interface Science*, vol. 361, 2, pp. 497-502, September 2011

[11] Y. S. Jung, J. Y. Lee, K. H. Ahn, and S. J. Lee, Effect of affinity on the structure formation in highly size asymmetric bimodal suspensions, *Colloids and Surfaces A: Physicochemical and Engineering Aspects*, vol. 538, pp. 481-487, February 2018

[12] J. Lee, S. J. Lee, K. H. Ahn, and S. J. Lee, Bimodal colloid gels of highly size-asymmetric particles, *Physcical Review E*, vol. 92, 1, July 2015

[13] S. Lim, S. Kim, K. H. Ahn, and S. J. Lee, The effect of binders on the rheological properties and the microstructure formation of lithium-ion battery anode slurries, *Journal of Power Sources,* vol. 299, pp. 221-230, December 2015

[14] S. Lim, S. Kim, K. H. Ahn, and S. J. Lee, Stress development of Li-Ion battery anode slurries during the drying process, *Ind. Eng. Chem. Res.*, vol. 54, 23, pp. 6146-6155, 2015

[15] J. A. Lewis, K. A. Blackman, A. L. Ogden, J. A. Payne, and L. F. Francis, Rheological property and stress development during drying of tape cast ceramic layers, *Journal of the American Ceramic Society*, vol. 79, 12, pp. 3225-3234, December 1996

[16] L. F. Francis, A. V. Mccormick, D. M. Vaessen, and J. A. Payne, Development and measurement of stress in polymer coatings, *Journal of Materials Science*, vol. 37, 22, pp. 4717-4731, November 2002

[17] K. B. Singh, and M. S. Tirumkudulu, Cracking in drying colloidal films, *Physical Review Letters*, vol. 98, May 2007

[18] E. M. Corcoran, Determining stresses in organic coatings using plate beam deflection, *Journal of Paint Technology*, vol. 41, pp. 635-640, 1969

[19] C. Lia, J. Leeb, C. Loa, and M. Wu, Effects of PAA-NH4 addition on the dispersion property of aqueous LiCoO2 slurries and the cell performance of as-prepared LiCoO2 cathodes, *Electrochemical and Solid-State Letters*, vol. 8, 10, A509-A512, 2005

[20] T. Swift, L. Swanson, M. Geoghegan, and S. Rimmer, The pH-responsive behaviour of poly(acrylic acid) in aqueous solution is dependent on molar mass, *Soft Matter*, vol. 12, pp. 2542-2549, 2016

[21] P. Wedin, C. J. Martinez, J. A. Lewis, J. Daicic, L. Bergström, Stress development during drying of calcium carbonate suspensions containing carboxymethylcellulose and latex particles, *Journal of colloid and interface science,* vol. 272, 1, pp. 1-9, April 2004

[22] D. J. Shaw, The solid－gas interface. Introduction to Colloid and Surface Chemistry, 4th

ed. Butterworth-Heinemann Ltd.: London, 1992

[23] P. Wedin, J. A. Lewis, L. Bergström, Soluble organic additive effects on stress development during drying of calcium carbonate suspensions, Journal of Colloid and Interface Science, vol. 290, 1, pp. 134-144, October 2005

[24] S. Lim, S. Kim, K. H. Ahn, and S. J. Lee, Stress development of Li-Ion battery anode slurries during the drying process, Ind. Eng. Chem. Res., vol. 54, 23, pp 6146–6155, 2015

[25] R. Y. Z. Hu, A. T. A. Wang, and J. P. Hartnett, Surface tension measurement of aqueous polymer solutions, Experimental Thermal and Fluid Science, vol. 4, 6, pp. 723-729, 1991

[26] B. Bitsch, T. Gallasch, M. Schroeder, M. Börner, M. Winter, and N. Willenbacher, Capillary suspensions as beneficial formulation concept for high energy density Li-ion battery electrodes, Journal of Power Sources, vol. 328, pp. 114-123, October 2016

# 국문 초록

리튬 이온 전지는 고 에너지 밀도의 전지이자 긴 cycle life을 가지고 있어서 그 필요성이 점점 증가하고 있다. 전극 공정과 관련하여, 입자를 개질하여 전극 성능을 향상시키거나 단위 공정의 변수들을 바꿔 공정을 최적화하거나 슬러리 상태에서 각 성분의 성분비 및 interaction을 변화시켜 유변 물성을 조절하는 연구들이 진행되어 왔다. 하지만 고분자 바인더와 활물질 사이의 interaction 변화를 기반으로, 슬러리 상태와 건조 후 미세구조의 관련성을 알아보는 연구는 많이 진행되지 않았다. 따라서 본 연구에서는 고분자 바인더로 poly(acrylic acid) (PAA)를 사용한 수계 음극 슬러리에서 pH에 따른 흡착 정도가 건조 거동과 건조 후 미세구조에 어떤 영향을 미치는지를 다루었다. PAA와 마이크로 사이즈의 활물질인 graphite를 기반으로 한 슬러리의 pH를 각각 3, 7, 11로 조절하여 흡착량을 측정하였을 때 pH가 높아질수록 흡착량이 감소하며, pH 11의 슬러리는 흡착량이 0임을 알 수 있었다. Interaction 차이가 존재함을 흡착량 측정 실험으로 확인한 후, 일정한 조건에서 각 슬러리를 건조시켜 건조 거동의 차이를 확인하였다. pH가 11일 때 건조 중간에서 peak이 발생했으며 이 peak의 발생은 capillary stress로 인한 것임을 접촉각 및 표면장력 실험을 통해서 확인하였다. 이에 반해 pH가 더 낮은 슬러리는 polymer shrinkage로 인한 maximum plateau region만 존재함을 확인했다. 건조 후 미세구조를 알 수 있는 공극률 측정 실험에서도, pH 11의 슬러리로 제조된 전극은 나노 사이즈의 pore가 없을 뿐만 아니라 공극률도 다른 슬러리에 비해 낮음을 확인할 수 있었다. 전극 슬러리의 흡착 정도를 조절하면 건조 공정과 전극의 미세구조에도 영향을 주기 때문에 이를 잘 활용하면 생산성 향상을 기대

할 수 있을 것이다.